Hindawi
Journal of Chemistry
Volume 2017, Article ID 7365263, 9 pages
https://doi.org/10.1155/2017/7365263

Research Article

Photodynamic Efficiency of Xanthene Dyes and Their Phototoxicity against a Carcinoma Cell Line: A Computational and Experimental Study

Suelen T. G. Buck,[1] Fernanda Bettanin,[2] Ednilson Orestes,[3] Paula Homem-de-Mello,[2] Hidetake Imasato,[1] Rommel B. Viana,[1] Janice R. Perussi,[1] and Albérico B. F. da Silva[1]

[1]*Departamento de Química e Física Molecular, Instituto de Química de São Carlos, Universidade de São Paulo, São Carlos, SP, Brazil*
[2]*Centro de Ciências Naturais e Humanas, Universidade Federal do ABC, Santo André, SP, Brazil*
[3]*Escola de Engenharia Industrial Metalúrgica de Volta Redonda, Departamento de Ciências Exatas, Universidade Federal Fluminense, Volta Redonda, RJ, Brazil*

Correspondence should be addressed to Paula Homem-de-Mello; paula.mello@ufabc.edu.br, Rommel B. Viana; rommelbv@yahoo.com.br, Janice R. Perussi; janice@iqsc.usp.br, and Albérico B. F. da Silva; alberico@iqsc.usp.br

Received 19 August 2016; Accepted 21 November 2016; Published 12 February 2017

Academic Editor: Teodorico C. Ramalho

The aim of this study is to assess the insights of molecular properties of the xanthene dyes [fluorescein (**FL**), Rose Bengal (**RB**), erythrosin B (**EB**), and eosin Y (**EY**)] to correlate systematically their photodynamic efficiency as well as their phototoxicity against a carcinoma cell line. The phototoxicity was evaluated by comparing the values of the medium inhibitory concentration (IC_{50}) upon HEp-2 cells with the xanthene corresponding photodynamic activity using the uric acid as a chemical dosimeter and their octanol-water partition coefficient (log *P*). **RB** was the more cytotoxic dye against HEp-2 cell line and the most efficient photosensitizer in causing photoxidation of uric acid; nevertheless it was the only one characterized as being hydrophobic among the xanthenes studied here. On the other hand, it was observed that the halogen substituents increased the hydrophilicity and photodynamic activity, consistent with the cytotoxic experiments. Furthermore, the reactivity index parameters, electric dipole moment, molecular volume, and the frontier orbitals were also obtained by the Density Functional Theory (DFT). The lowest dipole moment and highest molecular volume of **RB** corroborate with its highest hydrophobicity due to heavy atom substituents like halogens, while the halogen substituents did not affect expressively the electronic features at all.

1. Introduction

The photodynamic therapy (PDT) is a promising cancer treatment that involves the systemic or topic administration of a photosensitizer followed by a period of time in which the PS accumulates preferentially in the tumors cells followed by irradiation with visible light of compatible wavelength and absorption of the photosensitizer. Each factor is harmless by itself but when combined with molecular oxygen leads to the generation of lethal cytotoxic species and consequently to cell death and tissue destruction [1–4]. The photodynamic therapy is an interesting treatment for cancer due to dual selectivity produced by both preferential uptake of the photosensitizer by the diseased tissue and the ability to confine activation of the photosensitizer to this diseased tissue by restricting the illumination to that specific region. Therefore, PDT allows for the selective destruction of tumors while leaving normal tissue intact [1–5].

Photofrin®, a complex mixture of porphyrin monomers, dimmers, and oligomers, was the first compound approved by the Food and Drug Administration (FDA) to be used in PDT for the treatment of some types of cancer. Although

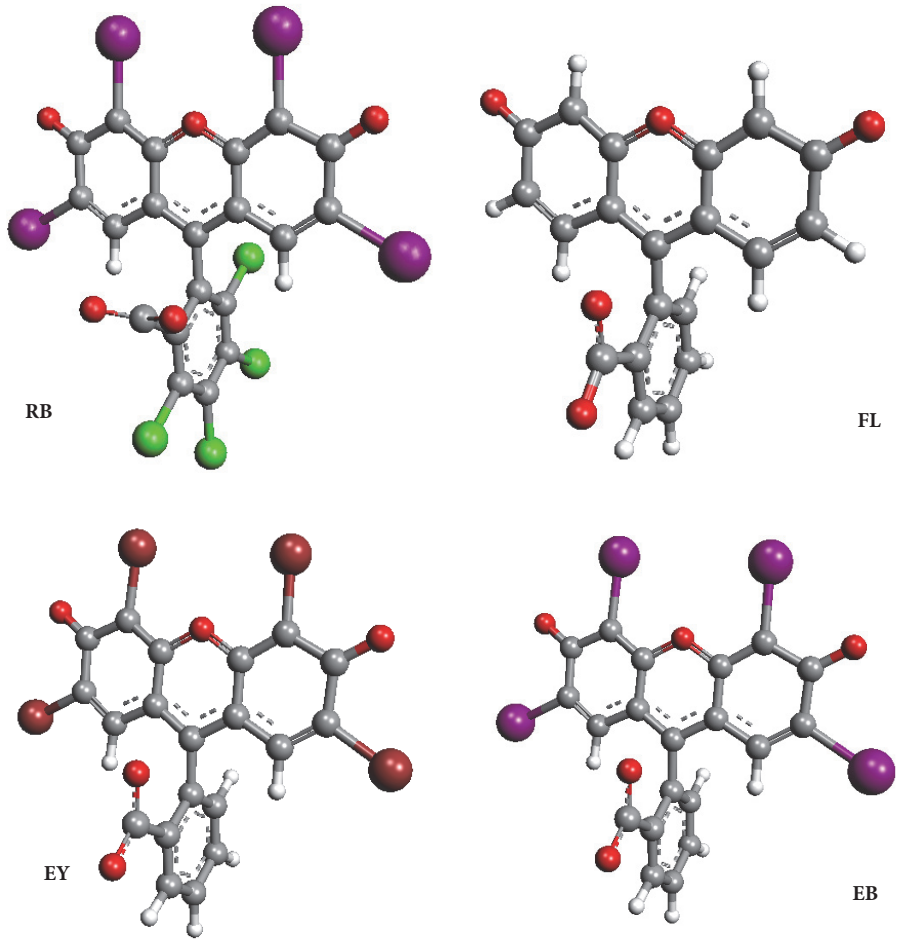

Figure 1: The optimized structures of the four xanthene dyes with B3LYP/6-31+G(d). The xanthene dyes: Rose Bengal (**RB**), erythrosin B (**EB**), eosin Y (**EY**), and fluorescein (**FL**).

Photofrin and other porphyrin-related sensitizers show a weak absorbance in the red region of the spectrum (≥600 nm), where penetration of light in tissue is optimal, these sensitizers induce long-lasting skin photosensitivity (4–6 weeks) through retention in cutaneous tissue [6–8]. Hence, the search for pure photosensitizers with light absorption in the range of 600 nm or higher, together with the absence of side effects exhibited by Photofrin, has led to the search and development of series of compounds, including chlorins and phtalocyanines with adequate absorption coefficients, that is, above 650 nm [6–8].

In order to understand the mechanisms involved in PDT, so that more effective photosensitizers can be developed, some synthetic xanthene dyes have been considered. That is the case of cyclic anionic xanthene dyes with three aromatic rings in linear arrangement and an atom of oxygen in the central ring as, for example, Rose Bengal (**RB**), erythrosin B (**EB**), eosin Y (**EY**), and fluorescein (**FL**) (Figure 1). These dyes possess interesting properties for PDT such as considerable quantum yield of singlet oxygen, intense light absorption in the visible region of the spectrum (500–570 nm), and low costs. Moreover, since these dyes do not absorb light in the wavelength of maximum tissue penetration (600–900 nm), they have been indicated for the treatment of superficial injuries [9–11].

Rose Bengal is known to produce singlet oxygen with a quantum yield of nearly 100% under illumination [12–14]. It is also reported that the Rose Bengal induces damage in rabbit corneal (in vitro) [13] and in retinal pigment epithelial cells [15]. Notwithstanding, **RB** shows a high potential to be used as photosensitizer and its clinical application has been limited since **RB** is immediately excreted right after being introduced into the living body and accumulated in the liver [12, 13, 15]. In addition, **RB** has been used topically in ophthalmology for diagnoses and in photodynamic inactivation of different microorganisms [14, 16–18]. On the other hand, erythrosin B and eosin Y possess photodynamic activity on bacteria and yeast [10, 16, 17, 19]. In the case of fluorescein, it shows high fluorescence making it an ideal visualizing agent for optical diseases leading as corneal trauma detection [20]; however it is not therapeutically used due to its low toxicity.

The interest in these dyes continues to be new as their derivatives are still nowadays being prepared and intensely studied. For example, Rose Bengal acetate [21] improves

diagnostics and therapeutic effects due to the addition of a quencher group [21–32]. Other examples are the investigation of fluorescein [33], erythrosin [34], and eosin derivatives [35] that have favorable characteristics for use in photodynamic therapy. Therefore, the photodynamic efficiency of four xanthene dyes (Rose Bengal, erythrosin B, eosin Y, and fluorescein) was determined in the present study by comparing their medium inhibitory concentration (IC_{50}) values in HEp-2 cells, their photodynamic activity using uric acid as a chemical dosimeter, and their octanol-buffer partition coefficient ($\log P$). These results were then related to molecular and electronic properties of these dyes obtained with Density Functional Theory (DFT) aiming to provide insights for a rational design of new and better compounds to be used as photosensitizers in PDT [36–41].

2. Materials and Methods

2.1. Photosensitizers and Light Source. The xanthene dyes Rose Bengal, erythrosin B, eosin Y, and fluorescein, the reagents 3-(4,5-dimethylthiazol-2-yl)-2,5-diphenyltetrazolium bromide (MTT) and 1-octanol, were purchased from Sigma-Aldrich and were used without further purification. The dyes stock solutions were made by weighting and diluting (until the desired concentrations) using phosphate buffered saline (PBS) and storing at 4°C in the dark. The green light source was a BIOTABLE containing an array of diode emitting light (LED) at 532 nm providing a fluence rate of 19 mW cm^{-2}.

2.2. Cell Culture. The human larynx carcinoma cell line (HEp-2, CCL-23™) used in this study was grown in ISCOVE'S medium (Sigma) containing 10% fetal calf serum and streptomycin (10 000 μg/mL)/penicillin (10 000 units mL^{-1}) (Sigma) as monolayers adhered to the plastic bottles at 37°C, 5% CO_2, and 95% air atmosphere.

2.3. Phototoxicity and Dark Toxicity. In order to study the intrinsic cellular toxicity of xanthene dyes, the cells were harvested using trypsin and incubated overnight for complete cell adhesion in 96-well plates at a concentration of 1×10^5 cells mL^{-1} (2 mL $well^{-1}$). A range of concentrations of the dyes were added and incubated for 6 h. The medium with the dyes was then removed and fresh medium was added. For phototoxicity measurements, plates were illuminated with LED at 532 nm for 15 min, giving a light dose of 18 J cm^{-2}. Following this treatment, the cells were maintained at 37°C, 5% CO_2, and 95% air for additional 48 h. To evaluate cell viability and thus calculate the toxicity, 50 μL of MTT was added to each well and this was incubated for 3 h [42]. The medium and MTT were aspirated; then 50 μL of ethanol and 150 μL of a solution containing PBS and 2-propanol were added to each well in order to solubilize the crystals. The absorbance was read on a plate reader (Benchmark-BIO-RAD) at 570 nm.

2.4. Photodynamic Activity (PA). Uric acid (UA) is a known singlet oxygen scavenger used as a chemical dosimeter to determine the photodynamic activity of photosensitizers, since this parameter is related to quantum yields for singlet oxygen production. When a solution of uric acid and photosensitizer is irradiated, the uric acid absorption band at 292 nm decreases as an evaluation of relative photodynamic activity of the photosensitizer [43–45]. The samples containing 10 μg mL^{-1} of uric acid and 5 μg mL^{-1} of the photosensitizer were irradiated with green LED during 360 s. Before and after the irradiation, the absorbance spectra were registered and photodynamic activity could be determined by Fischer's expression [44]:

$$\mathrm{PA} = \frac{\Delta A_{\mathrm{UA}} \cdot 10^5}{E_0 t A_{\mathrm{PS}\,\lambda\mathrm{irr}}}, \tag{1}$$

where PA is the photodynamic activity ($m^2\,J^{-1}$), ΔA_{UA} is the absorbance decrease at 292 nm in a mixture of uric acid and photosensitizer after irradiation, E_0 is the fluence rate ($W\,m^{-2}$), t is the irradiation time (s), and $A_{\mathrm{PS}.\lambda\mathrm{irr}}$ refers to the absorbance of the photosensitizer in uric acid and photosensitizer solution at irradiation wavelength.

2.5. Partition Coefficients. The partition coefficients ($\log P$) were taken as a measure of the hydrophobic character of the dyes. They were calculated using the method of Pooler and Valenzeno [46]. Phosphate buffered saline and 1-octanol were used as immiscible solvents initially saturated to each other. The dyes were dissolved in PBS (phosphate buffered saline) to give a final concentration of 3 μg mL^{-1}; then 10 mL of each of these solutions was individually placed in a flask with equal volume of 1-octanol. After 1 h of agitation, the mixture was left to rest overnight and then centrifuged. The dye concentration in PBS before and after being mixed with octanol was measured spectrophotometrically in a Hitachi U-2800. The logarithm of the partition coefficient, $\log P$, was calculated according to

$$\log P = \left[\left(\frac{A_B}{A_A}\right) - 1\right] \frac{V_{\mathrm{PBS}}}{V_{\mathrm{OCT}}}, \tag{2}$$

where A_B and A_A are the measured absorbance of the dye solution in PBS before and after partitioning, respectively. V_{PBS} and V_{OCT} are the volumes of the PBS and octanol phases, respectively. The partition coefficient was determined five times for each dye.

2.6. Computational Methodology. The chemical structure of the four xanthene dyes Rose Bengal, erythrosin B, eosin Y, and fluorescein studied in this work (Figure 1) was also investigated with Density Functional Theory (DFT) as implemented in Gaussian 03 package [47]. In the first step, a fully unconstrained geometry optimization was performed on the molecular structure of all xanthene dyes using B3LYP [48, 49] (Becke's three-parameter hybrid exchange functional and Lee, Yang, and Parr's correlation functional) and 6-31+G(d) basis sets [50, 51]. It was followed by a vibrational frequency analysis and the absence of imaginary frequencies was used as a criterion to ensure that each optimized structure corresponds to a true minimum on their respective potential energy surface. The solvent effects were treated with the Integral Equation Formulation of the Polarizable Continuum

Table 1: IC_{50} ($\mu g\,mL^{-1}$) values under illumination (light dose of 18 J cm^{-2}) and in the dark for the xanthene dyes incubated in HEp-2 cells for 6 h*.

Dye	IC_{50}	Dark-IC_{50}
Rose Bengal (**RB**)	11 ± 1	58 ± 2
Erythrosin B (**EB**)	74 ± 3	125 ± 10
Eosin Y (**EY**)	104 ± 7	135 ± 8
Fluorescein (**FL**)	370 ± 35	630 ± 60

*The fluorescence rate of the used LED was 19 mW cm^{-2}. The mean values and the standard deviations (m ± sd) for $n = 7$.

Table 2: Photodynamic activity ($m^2\,J^{-1}$) of the photosensitizers [the mean values and the standard deviations (m ± sd) for $n = 4$].

Dye	Photodynamic activity
Rose Bengal (**RB**)	6.0 ± 0.3
Erythrosin B (**EB**)	5.6 ± 0.5
Eosin Y (**EY**)	4.2 ± 0.6
Fluorescein (**FL**)	0.4 ± 0.1

Table 3: The partition coefficient values for the xanthene dyes studied [the mean values and the standard deviations (m ± sd) for $n = 5$].

Dye	log P
Rose Bengal (**RB**)	0.66 ± 0.01
Erythrosin B (**EB**)	−0.35 ± 0.04
Eosin Y (**EY**)	−0.65 ± 0.07
Fluorescein (**FL**)	−1.00 ± 0.02

Model (IEF-PCM) method [52–54] simulating the water environment, which has been successfully applied to study other tricyclic molecules [55, 56].

Once the optimized structures were properly obtained, the energies of frontier molecular orbitals HOMO (highest occupied molecular orbital) and LUMO (lowest unoccupied molecular orbital), as well as electric dipole moment, molecular electrostatic potential, area, and volume of the four xanthene dyes, were then calculated.

3. Results and Discussion

Table 1 shows the phototoxicity and dark toxicity of the xanthenes in HEp-2 after 6 h incubation with the dye. Under dark conditions, the tested dyes showed Dark-IC_{50} values indicating some level of inherent toxicity to this cell line. **RB** presented the highest levels of such toxicity with IC_{50} of 58 $\mu g\,mL^{-1}$, while **FL** showed the lowest intrinsic toxicity observed with IC_{50} of 630 $\mu g\,mL^{-1}$. It is important to comment that the incubation time affected the xanthene dyes cytotoxicity, where the decrease of the incubation time leads to an increase of the IC_{50} value, suggesting that more dyes accumulate in the cell.

Another inspection on Table 1 demonstrates that the light greatly improved the cytotoxicity of the dyes in the cell line tested. In this aspect, **RB** was found to be the most phototoxic dye with IC_{50} of 11 $\mu g\,mL^{-1}$, which was the lowest IC_{50} under illumination, followed by **EB**, **EY,** and **FL**, as shown by Masamitsu et al. [57]. In contrast, **FL** reaches 40% of its potentialization by light, whereas **RB** shows a large decreasing in IC_{50} under illumination (≈80%), which is compared with the other photosensitizers that reach their maximum potentialization in the used light dose.

Figure 2 shows the variation in absorbance bands assigned to uric acid (292 nm) and the minor changes at the absorption bands of the photosensitizers, probably due to some photodecomposition of the dyes. This method is based on the suppression of singlet oxygen by uric acid ($k = 3.6 \times 10^8$ mol L^{-1}), and it is important to mention that this reaction leads to formation of triuret, sodium oxalate, allantoxaidin, and CO_2, according to Fischer et al. [44]. In addition, Table 2 presents the obtained values for photodynamic activities. In the case of **RB**, this dye demonstrated the highest photodynamic activity result (6.0 m^2/J), while **FL** showed the lowest one (0.4 m^2/J). These results agree with the cytotoxic experiments, where the lowest and the highest IC_{50} values are detected by **RB** and **FL**, respectively. This relation is possible of verifying, once the singlet oxygen is considered the main responsible agent to cause tumor cells death and irradiated photosensitizers that produces higher amounts of singlet oxygen and consequently lead to high cytotoxic effects. Thus, the results of the photooxidation of uric acid and determination of the IC_{50} experiments converge to the following order of photodynamic efficiency for the dyes studied here: Rose Bengal (**RB**) > erythrosin B (**EB**) > eosin Y (**EY**) > fluorescein (**FL**).

Table 3 shows the logarithm of the partition coefficients of the photosensitizers. Here it is important to remember that the hydrophilic character of a compound is associated with the poor distribution in octanol/water (then log $P < 0$), while lipophilic substances are characterized by log $P > 1.5$. On the other hand, species that present log P in the intermediate range are considered amphiphilic [58]. Therefore, the log P results indicate **RB** as being amphiphilic ($0 <$ log $P <$ 1.5), while the other dyes demonstrate a hydrophilic nature (log P <0). These results are in agreement with the photodynamic activity and IC_{50} values, once **RB** is the most hydrophobic dye and demonstrated the highest photodynamic activity value being the most cytotoxic. **EB** and **EY** have high values of photodynamic activity (5.6 e 4.2 $m^2\,J^{-1}$) but they are not the most cytotoxic, being this result in agreement with log P values for these dyes, suggesting that they are hydrophilic and have the tendency to locate in plasma membrane. Nevertheless, a different picture is seen for **FL** which shows a hydrophilic character and possess the lowest value of photodynamic activity (0.4 m^2 J), which may explain the fact of being the least efficient photosensitizer among the dyes studied here. This hydrophilic/lipophilic balance of the photosensitizer is very important in determining its cell localization and therefore its site of action [59–61], where a hydrophobic photosensitizer can diffuse across the plasma membrane and then to relocate to other intracellular membranes. In contrast, those ones that are less hydrophobic

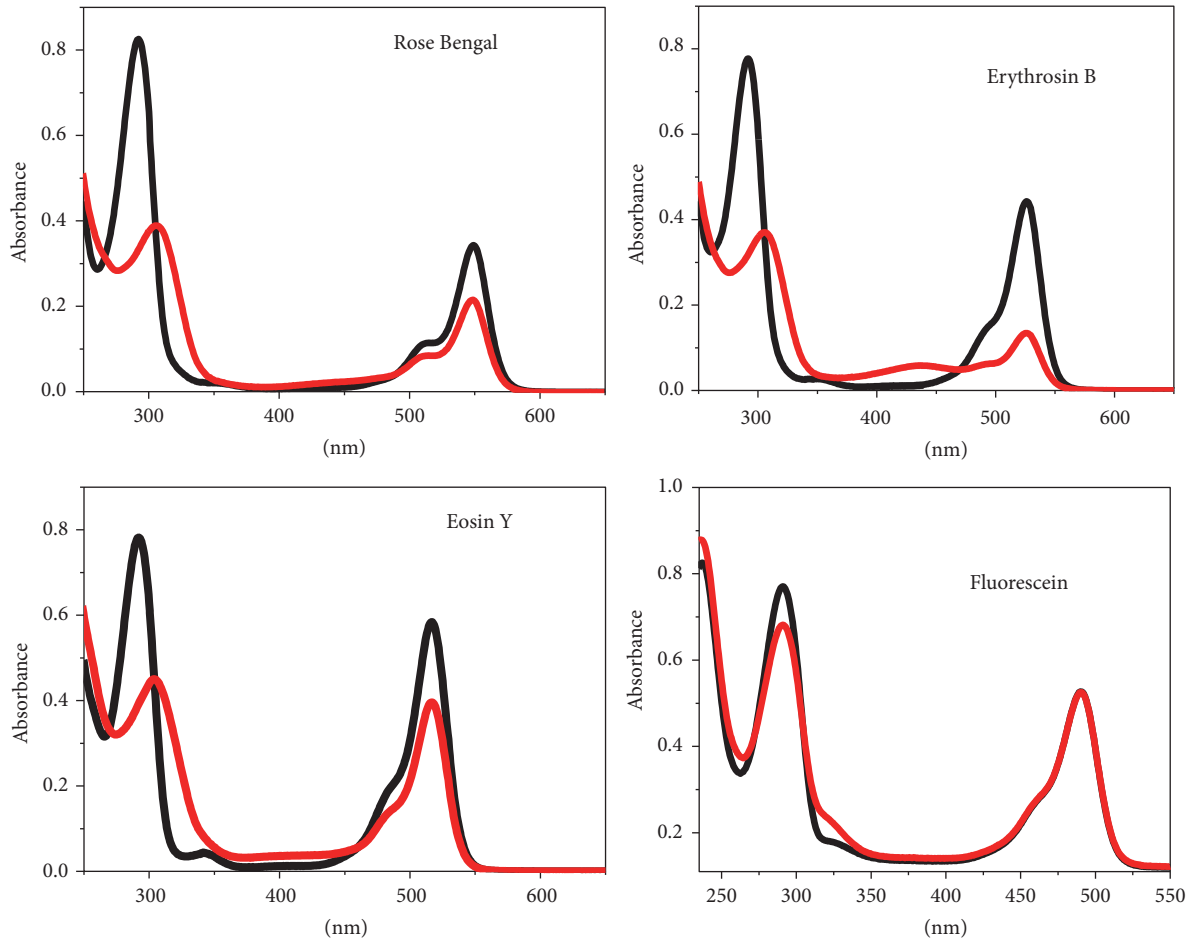

Figure 2: Absorption spectra of solutions containing uric acid (10 μg mL^{-1}) and dye (5 μg mL^{-1}) dissolved in PBS before (black) and after (red) the irradiation with LED. The absorption spectra show the decrease of the band in 292 nm attributed to the acid uric photoxidation.

tend to be too polar to diffuse across the plasma membrane, having its action restricted to this site, or are taken up by endocytosis [61]. Moreover, lipophilic photosensitizer tends to be localized in the mitochondria [62, 63] and the activation of a photosensitizer located in the mitochondria leads to apoptosis [59, 64].

From another glance at Figure 1, it can be seen that the 3-oxo-xanthen-9-yl system is planar in all cases and the angle between this plane and the phenyl ring is *ca.* 60° for **EB**, **EY**, and **FL** while **RB** shows a right angle possibly due to hindrance effect of the ortho-chlorine atoms bonded to the phenyl ring. In addition, plots of the frontier molecular orbitals are presented in Figure 3. The HOMO plots are very similar for all xanthene dyes studied, except for the different contributions of carboxylic acid group bonded to the phenyl ring. The atoms localized at the extremity of 3-oxo-xanthen-9-yl ring system contribute to the HOMO of all systems, while the HOMO of the **RB** and **EB** also shows contribution from the carboxylic acid group. The LUMO shows contributions from the atoms of the center of the 3-oxo-xanthen-9-yl ring system, while the oxygen atom from the carboxylic group of the **EB**, **EY,** and **FL**, positioned next to the 3-oxo-xanthen-9-yl ring system, also contributes to the LUMO of these systems. For the **RB** and **EB**, all iodine atoms participate in HOMO but not in LUMO. The same occurs to the bromine atoms of **EY**. Hence, the main transition (HOMO-LUMO) for the dyes studied in this work corresponds to a charge transfer from the extremity, including the substituent atoms, to the center of the ring system. Meanwhile, the LUMO plots depend on the compound. For example, only the LUMO of the **FL** shows contribution from the atoms of the substituents at three phenyl rings, while the 3-oxo-xanthen-9-yl ring system atoms are more important for the LUMO of the **EB** than for the LUMO of the **EY**.

The calculation of the reactivity index parameters was also performed based on the methodology of Pearson [65] and Parr et al. [66]. Table 4 presents the chemical hardness (η), electronic chemical potential (μ), electrophilicity (ω), and the Kohn-Sham eigenvalue of HOMO and LUMO. An interesting aspect in **RB** and **EB** is their small HOMO-LUMO gap energy, which may be caused from the stabilization induced by the iodine substituents over the tricyclic moiety that induces the electron-acceptor effect in these molecules. An interesting aspect is that the chloride atoms of the **RB** participate neither in the HOMO nor in the LUMO of this system indicating that the phenyl ring substituents do not contribute to increase of its HOMO-LUMO energy gap. The η result is an important indication of the resistance of

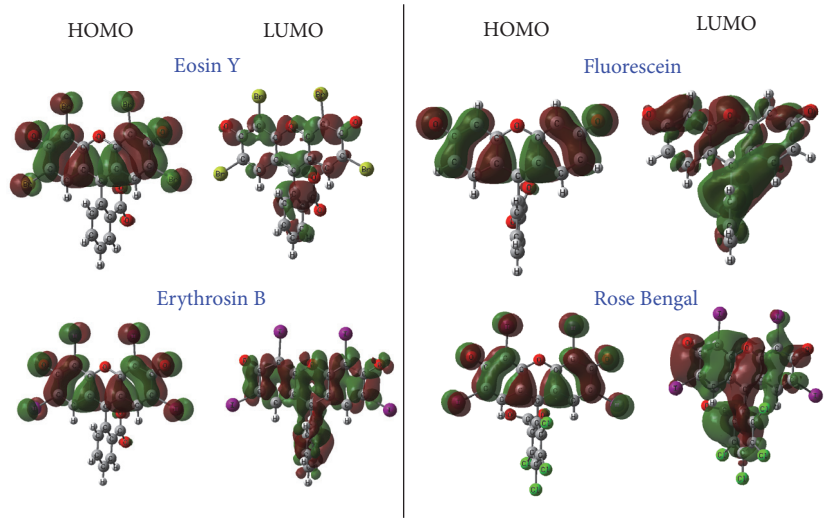

Figure 3: Plots of frontier orbitals (HOMO and LUMO) for the four xanthene dyes studied.

Table 4: The HOMO and LUMO energies (in eV), HOMO-LUMO energy gap (in eV), the chemical hardness (η, in eV), electronic chemical potential (μ, in eV), electrophilicity (ω, in eV), the area (Å^2), volume (Å^3), and electric dipole moment (in Debye) for each xanthene dye studied.

Properties	FL	EB	EY	RB
HOMO	−5.1	−0.7	−5.5	−0.9
LUMO	−2.1	−0.4	−2.5	−0.9
Gap	−3.0	−0.3	−3.0	0.0
μ	3.6	0.6	4.0	0.9
η	3.0	0.3	3.0	0.0
ω	2.2	0.6	2.7	1.0
Area	510.1	660.1	626.4	732.7
Volume	859.0	1169.2	1090.4	1317.1
Dipole	16.7	12.2	14.2	11.2

compounds to change its electronic configuration, while μ is a parameter to predict the escaping tendency of electrons in the specie, which is also associated with the electronic charge rearrangement associated with any chemical process. Among the four structures, the lowest η value is estimated for **RB**, while the lowest μ result is seen for **EB**. In addition, it is noted that **EB** shows a better electrophilic character than the other dyes examining the electrophilicity index, while **FL** and **EY** showed a large nucleophilic character. In general aspects, severe changes are not observed when we compare **FL**/**EY** or even **EB**/**RB**. Moreover, this large nucleophilic nature from **FL** and **EY** may also explain the fact that these two dyes present the highest IC_{50} results.

Since the area and the molecular volume are directly related to the experimental data (i.e., **RB** > **EB** > **EY** ≫ **FL**), the photodynamic activity decreases from **RB** to **FL** due to the presence of heavy atoms. It has been often demonstrated that the replacement of an atom in a structure by other with higher atomic number leads to an increase of the quantum yield. The hydrophilic/lipophilic character of the molecules can be evaluated by means of the quantum chemical calculations from the following properties: dipole moments, atomic charges, area, and molecular volumes. The dipole moment results show that **RB** has the lowest dipole moment obtained, what could be assigned to the presence of chloride atoms, which present negative charges. As the 3-oxo-xanthen-9-yl ring system essentially does not contribute to the **RB** dipole moment, this is the most hydrophobic molecule explaining its highest log P value. Contrarily, the results presented in this work indicate that the presence of heavy atoms does not change the electronic properties of the dyes studied but increases their hydrophobicity as demonstrated by the decrease in the electric dipole moments (**FL** > **EY** > **EB** > **RB**), whereas in addition an increase in the molecular volume is estimated (**RB** > **EB** > **EY** ≫ **FL**).

Another important issue, which needs to be addressed here, is the molecular electrostatic potential as presented in Figure 4. Examining **RB**, the nucleophilic and the electrophilic regions are localized in the phenyl group and in the peripheral areas, respectively. In **RB**, a different picture is noted when we look at the central region, where the neutral area is localized with a small point presenting a nucleophilic character. In contrast, **EB** shows a similar picture with **RB**; however **EB** demonstrates a decrease in the nucleophilic nature of the phenyl group, whereas in the central area a large positive region is observed. Nevertheless, **FL** and **EY** present a neutral region around each molecule with a large negative area in the carboxyl group. Thus, the neutral/nucleophilic character at the phenyl group may explain the interaction with uric acid and the photocytotoxicity assay. On the other hand, it does not mean, however, that **RB** and **EB** should show similar behavior as photosensitizers, since the presence of the chloride atoms is the only difference in the composition of these compounds. As the presence of the chloride atoms is the only difference in the composition of **RB** and **EB**, it does not mean that these compounds should present similar behavior as photosensitizers

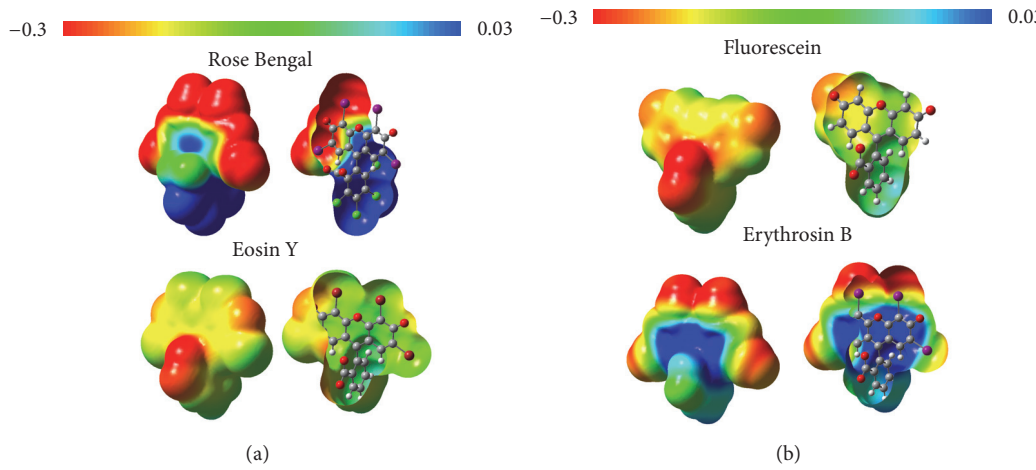

FIGURE 4: Molecular electrostatic potential of each xanthene dye (isovalue of 0.0004 a.u.). The right-side view shows the front of the solid surface, and the left-side view shows the back of the surface and displays its molecular disposition. The regions in red refer to areas with an electrophilic character, while the regions in blue are areas with a nucleophilic nature. A different case is the area in green which is related to neutral regions.

since the intrinsic characteristics of these chloride atoms can significantly change other properties of **RB** such as aggregation and volume, hence altering their efficiency in photodynamic activity. Moreover, as **RB** shows higher photodynamic efficiency than **EB**, the presence of iodine atoms could be even better substituent instead of chloride.

4. Conclusions

The purpose of this investigation was to perform an assessment of two methods in order to characterize the photodynamic efficiency of four dyes with potential use in photodynamic therapy. The medium inhibitory concentration (IC_{50}) in tumoral cell line HEp-2 was determined aiming to evaluate the dyes cytotoxicity and phototoxicity. The photoxidation of uric acid was used to estimate the production of singlet oxygen of the dyes, while the determination of the octanol-buffer partition coefficient ($\log P$) allowed measuring the lipophilic character of the compounds considered. **RB** showed the higher phototoxicity among the xanthene dyes studied in this work; however this dye has the highest toxicity without illumination against Hep-2. Although the other dyes are less effective in killing cells under illumination, they have much lower intrinsic dark cytotoxicity. Moreover, a quantum chemical investigation was also carried out to provide valuable insights for the design of new and better compounds to be employed as photosensitizers in photodynamic therapy.

Competing Interests

The authors declare that there are no competing interests regarding the publication of this paper.

Acknowledgments

The authors are grateful for the financial support given by the Brazilian agencies CNPq, CAPES, and FAPESP (11/09979-4; 07/05370-0; 10/19790-3; 12/19175-2). Fernanda Bettanin and Rommel B. Viana also wish to thank CAPES for the research fellowships.

References

[1] W. M. Sharman, C. M. Allen, and J. E. Van Lier, "Photodynamic therapeutics: basic principles and clinical applications," *Drug Discovery Today*, vol. 4, no. 11, pp. 507–517, 1999.

[2] E. Buytaert, M. Dewaele, and P. Agostinis, "Molecular effectors of multiple cell death pathways initiated by photodynamic therapy," *Biochimica et Biophysica Acta—Reviews on Cancer*, vol. 1776, no. 1, pp. 86–107, 2007.

[3] A. P. Castano, T. N. Demidova, and M. R. Hamblin, "Mechanisms in photodynamic therapy: part two—cellular signaling, cell metabolism and modes of cell death," *Photodiagnosis and Photodynamic Therapy*, vol. 2, no. 1, pp. 1–23, 2005.

[4] D. E. J. G. J. Dolmans, D. Fukumura, and R. K. Jain, "Photodynamic therapy for cancer," *Nature Reviews Cancer*, vol. 3, no. 5, pp. 380–387, 2003.

[5] Y. N. Konan, R. Gurny, and E. Allémann, "State of the art in the delivery of photosensitizers for photodynamic therapy," *Journal of Photochemistry and Photobiology B: Biology*, vol. 66, no. 2, pp. 89–106, 2002.

[6] R. R. Allison, G. H. Downie, R. Cuenca, X. Hu, C. J. Childs, and C. H. Sibata, "Photosensitizers in clinical PDT," *Photodiagnosis and Photodynamic Therapy*, vol. 1, no. 1, pp. 27–42, 2004.

[7] M. R. Detty, S. L. Gibson, and S. J. Wagner, "Current clinical and preclinical photosensitizers for use in photodynamic therapy," *Journal of Medicinal Chemistry*, vol. 47, no. 16, pp. 3897–3915, 2004.

[8] I. Walker, S. A. Gorman, R. D. Cox, D. I. Vernon, J. Griffiths, and S. B. Brown, "A comparative analysis of phenothiazinium salts for the photosensitisation of murine fibrosarcoma (RIF-1) cells *in vitro*," *Photochemical and Photobiological Sciences*, vol. 3, no. 7, pp. 653–659, 2004.

[9] Z. Diwu and J. William Lown, "Phototherapeutic potential of alternative photosensitizers to porphyrins," *Pharmacology and Therapeutics*, vol. 63, no. 1, pp. 1–35, 1994.

[10] H. Wang, L. Lu, S. Zhu, Y. Li, and W. Cai, "The phototoxicity of xanthene derivatives against *Escherichia coli, Staphylococcus aureus*, and *Saccharomyces cerevisiae*," *Current Microbiology*, vol. 52, no. 1, pp. 1–5, 2006.

[11] N. Uesugi, K. Furumiya, and T. Mizutani, "Inhibition mechanism of UDP-glucuronosyltransferase 1A6 by xanthene food dyes," *Journal of Health Science*, vol. 52, no. 5, pp. 549–557, 2006.

[12] N. Sugita, K.-I. Kawabata, K. Sasaki, I. Sakata, and S.-I. Umemura, "Synthesis of amphiphilic derivatives of rose bengal and their tumor accumulation," *Bioconjugate Chemistry*, vol. 18, no. 3, pp. 866–873, 2007.

[13] C.-C. Chang, Y.-T. Yang, J.-C. Yang, H.-D. Wu, and T. Tsai, "Absorption and emission spectral shifts of rose bengal associated with DMPC liposomes," *Dyes and Pigments*, vol. 79, no. 2, pp. 170–175, 2008.

[14] T. P. Paulino, K. F. Ribeiro, G. Thedei Jr., A. C. Tedesco, and P. Ciancaglini, "Use of hand held photopolymerizer to photoinactivate Streptococcus mutans," *Archives of Oral Biology*, vol. 50, no. 3, pp. 353–359, 2005.

[15] F. Nakonechny, M. Nisnevitch, Y. Nitzan, and M. Nisnevitch, "Sonodynamic excitation of rose bengal for eradication of gram-positive and gram-negative bacteria," *BioMed Research International*, vol. 2013, Article ID 684930, 7 pages, 2013.

[16] J. R. Perussi, "Inativação fotodinâmica de microrganismos," *Química Nova*, vol. 30, no. 4, pp. 988–994, 2007.

[17] J. R. Perussi and H. Imasato, "Inativação fotodinâmica de microrganismos," in *Novas Técnicas Ópticas Para as Áreas da Saúde*, V. Bagnato, Ed., vol. 1, pp. 163–183, São Carlos, Brazil, Livraria da Física, 2008.

[18] M. Schäfer, C. Schmitz, R. Facius et al., "Systematic study of parameters influencing the action of rose bengal with visible light on bacterial cells: comparison between the biological effect and singlet-oxygen production," *Photochemistry and Photobiology*, vol. 71, no. 5, pp. 514–523, 2000.

[19] D. Gao, Y. Tian, F. Liang et al., "Investigation on the pH-dependent binding of Eosin Y and bovine serum albumin by spectral methods," *Journal of Luminescence*, vol. 127, no. 2, pp. 515–522, 2007.

[20] M. Wainwright, "The use of dyes in modern biomedicine," *Biotechnic & Histochemistry*, vol. 78, no. 3-4, pp. 147–155, 2009.

[21] E. Panzarini, V. Inguscio, G. M. Fimia, and L. Dini, "Rose bengal acetate photodynamic therapy (RBAc-PDT) induces exposure and release of Damage-Associated Molecular Patterns (DAMPs) in human HeLa cells," *PLOS ONE*, vol. 9, no. 8, Article ID e105778, 2014.

[22] P. Agostinis, K. Berg, K. A. Cengel et al., "Photodynamic therapy of cancer: an update," *CA: A Cancer Journal for Clinicians*, vol. 61, no. 4, pp. 250–281, 2011.

[23] M. Korbelik, J. Sun, and I. Cecic, "Photodynamic therapy-induced cell surface expression and release of heat shock proteins: relevance for tumor response," *Cancer Research*, vol. 65, no. 3, pp. 1018–1026, 2005.

[24] F. Zhou, D. Xing, and W. R. Chen, "Dynamics and mechanism of HSP70 translocation induced by photodynamic therapy treatment," *Cancer Letters*, vol. 264, no. 1, pp. 135–144, 2008.

[25] S. Mitra, B. R. Giesselman, F. J. De Jesús-Andino, and T. H. Foster, "Tumor response to mTHPC-mediated photodynamic therapy exhibits strong correlation with extracellular release of HSP70," *Lasers in Surgery and Medicine*, vol. 43, no. 7, pp. 632–643, 2011.

[26] N. Etminan, C. Peters, D. Lakbir et al., "Heat-shock protein 70-dependent dendritic cell activation by 5-aminolevulinic acid-mediated photodynamic treatment of human glioblastoma spheroids *in vitro*," *British Journal of Cancer*, vol. 105, no. 7, pp. 961–969, 2011.

[27] E. Panzarini, B. Tenuzzo, F. Palazzo, A. Chionna, and L. Dini, "Apoptosis induction and mitochondria alteration in human HeLa tumour cells by photoproducts of Rose Bengal acetate," *Journal of Photochemistry and Photobiology B: Biology*, vol. 83, no. 1, pp. 39–47, 2006.

[28] E. Panzarini, B. Tenuzzo, and L. Dini, "Photodynamic therapy-induced apoptosis of HeLa cells," *Annals of the New York Academy of Sciences*, vol. 1171, pp. 617–626, 2009.

[29] E. Panzarini, V. Inguscio, and L. Dini, "Timing the multiple cell death pathways initiated by Rose Bengal acetate photodynamic therapy," *Cell Death & Disease*, vol. 2, no. 6, article e169, 2011.

[30] E. Panzarini, V. Inguscio, and L. Dini, "Overview of cell death mechanisms induced by rose bengal acetate-photodynamic therapy," *International Journal of Photoenergy*, vol. 2011, Article ID 713726, 11 pages, 2011.

[31] L. Dini, V. Inguscio, B. Tenuzzo, and E. Panzarini, "Rose bengal acetate photodynamic therapy-induced autophagy," *Cancer Biology and Therapy*, vol. 10, no. 10, pp. 1048–1055, 2010.

[32] E. Panzarini, V. Inguscio, B. A. Tenuzzo, and L. Dini, "In vitro and in vivo clearance of rose bengal acetate-photodynamic therapy-induced autophagic and apoptotic cells," *Experimental Biology and Medicine*, vol. 238, no. 7, pp. 765–778, 2013.

[33] T. A. Robertson, F. Bunel, and M. S. Roberts, "Fluorescein derivatives in intravital fluorescence imaging," *Cells*, vol. 2, no. 3, pp. 591–606, 2013.

[34] L. S. Herculano, G. V. B. Lukasievicz, E. Sehn et al., "Photodegradation in micellar aqueous solutions of erythrosin esters derivatives," *Applied Spectroscopy*, vol. 69, no. 7, pp. 883–888, 2015.

[35] B. M. Estevão, D. S. Pellosi, C. F. De Freitas et al., "Interaction of eosin and its ester derivatives with aqueous biomimetic micelles: evaluation of photodynamic potentialities," *Journal of Photochemistry and Photobiology A: Chemistry*, vol. 287, pp. 30–39, 2014.

[36] M. E. Alberto, C. Iuga, A. D. Quartarolo, and N. Russo, "Bisanthracene bis(dicarboxylic imide)s as potential photosensitizers in photodynamic therapy: a theoretical investigation," *Journal of Chemical Information and Modeling*, vol. 53, no. 9, pp. 2334–2340, 2013.

[37] É. Brémond, M. E. Alberto, N. Russo, G. Ricci, I. Ciofini, and C. Adamo, "Photophysical properties of NIR-emitting fluorescence probes: insights from TD-DFT," *Physical Chemistry Chemical Physics*, vol. 15, no. 25, pp. 10019–10027, 2013.

[38] M. E. Alberto, T. Marino, A. D. Quartarolo, and N. Russo, "Photophysical origin of the reduced photodynamic therapy activity of temocene compared to Foscan®: insights from theory," *Physical Chemistry Chemical Physics*, vol. 15, no. 38, pp. 16167–16171, 2013.

[39] M. E. Alberto, G. Mazzone, A. D. Quartarolo, F. F. R. Sousa, E. Sicilia, and N. Russo, "Electronic spectra and intersystem spin-orbit coupling in 1,2- and 1,3-squaraines," *Journal of Computational Chemistry*, vol. 35, pp. 2107–2113, 2014.

[40] G. Mazzone, A. D. Quartarolo, and N. Russo, "PDT-correlated photophysical properties of thienopyrrole BODIPY derivatives. Theoretical insights," *Dyes and Pigments*, vol. 130, pp. 9–15, 2016.

[41] G. Mazzone, M. Alberto, B. De Simone, T. Marino, and N. Russo, "Can expanded bacteriochlorins act as photosensitizers in photodynamic therapy? Good news from density functional theory computations," *Molecules*, vol. 21, no. 3, article no. 288, 2016.

[42] T. Mosmann, "Rapid colorimetric assay for cellular growth and survival: application to proliferation and cytotoxicity assays," *Journal of Immunological Methods*, vol. 65, no. 1-2, pp. 55–63, 1983.

[43] B. F. Becker, "Towards the physiological function of uric acid," *Free Radical Biology and Medicine*, vol. 14, no. 6, pp. 615–631, 1993.

[44] F. Fischer, G. Graschew, H.-J. Sinn, W. Maier-Borst, W. J. Lorenz, and P. M. Schlag, "A chemical dosimeter for the determination of the photodynamic activity of photosensitizers," *Clinica Chimica Acta*, vol. 274, no. 1, pp. 89–104, 1998.

[45] R. S. Cavalcante, H. Imasato, V. S. Bagnato, and J. R. Perussi, "A combination of techniques to evaluate photodynamic efficiency of photosensitizers," *Laser Physics Letters*, vol. 6, no. 1, pp. 64–70, 2008.

[46] J. P. Pooler and D. P. Valenzeno, "Physicochemical determinants of the sensitizing effectiveness for photooxidation of nerve membranes by fluorescein derivatives," *Photochemistry and Photobiology*, vol. 30, no. 4, pp. 491–498, 1979.

[47] M. J. Frisch, G. W. Trucks, H. B. Schlegel et al., *Gaussian 03, Revision B.04*, Gaussian, Inc, Wallingford, Conn, USA, 2004.

[48] C. Lee, W. Yang, and R. G. Parr, "Development of the Colle-Salvetti correlation-energy formula into a functional of the electron density," *Physical Review B*, vol. 37, no. 2, pp. 785–789, 1988.

[49] A. D. Becke, "Density-functional thermochemistry. III. The role of exact exchange," *The Journal of Chemical Physics*, vol. 98, no. 7, pp. 5648–5652, 1993.

[50] M. N. Glukhovtsev, A. Pross, M. P. McGrath, and L. Radom, "Extension of Gaussian-2 (G2) theory to bromine- and iodine-containing molecules: use of effective core potentials," *The Journal of Chemical Physics*, vol. 103, no. 5, pp. 1878–1885, 1995.

[51] V. A. Rassolov, M. A. Ratner, J. A. Pople, P. C. Redfern, and L. A. Curtiss, "6-31G* basis set for third-row atoms," *Journal of Computational Chemistry*, vol. 22, no. 9, pp. 976–984, 2001.

[52] E. Cancès, B. Mennucci, and J. Tomasi, "A new integral equation formalism for the polarizable continuum model: theoretical background and applications to isotropic and anisotropic dielectrics," *Journal of Chemical Physics*, vol. 107, no. 8, pp. 3032–3041, 1997.

[53] B. Mennucci, E. Cancès, and J. Tomasi, "Evaluation of solvent effects in isotropic and anisotropic dielectrics and in ionic solutions with a unified integral equation method: theoretical bases, computational implementation, and numerical applications," *The Journal of Physical Chemistry B*, vol. 101, no. 49, pp. 10506–10517, 1997.

[54] E. Cancès and B. Mennucci, "New applications of integral equations methods for solvation continuum models: ionic solutions and liquid crystals," *Journal of Mathematical Chemistry*, vol. 23, no. 3, pp. 309–326, 1998.

[55] P. Homem-de-Mello, B. Mennucci, J. Tomasi, and A. B. F. Da Silva, "The effects of solvation in the theoretical spectra of cationic dyes," *Theoretical Chemistry Accounts*, vol. 113, no. 5, pp. 274–280, 2005.

[56] R. A. De Toledo, M. C. Santos, H. B. Suffredini, P. Homem-de-Mello, K. M. Honório, and L. H. Mazo, "DFT and electrochemical studies on nortriptyline oxidation sites," *Journal of Molecular Modeling*, vol. 15, no. 8, pp. 945–952, 2009.

[57] T. Masamitsu, M. Kinoshita, Y. Yoshihara et al., "Optimal photosensitizers for photodynamic therapy of infections should kill bacteria but spare neutrophils," *Photochemistry and Photobiology*, vol. 88, no. 1, pp. 227–232, 2012.

[58] M. Wainwright and R. M. Giddens, "Phenothiazinium photosensitisers: choices in synthesis and application," *Dyes and Pigments*, vol. 57, no. 3, pp. 245–257, 2003.

[59] D. A. Phoenix, Z. Sayed, S. Hussain, F. Harris, and M. Wainwright, "The phototoxicity of phenothiazinium derivatives against *Escherichia coli* and *Staphylococcus aureus*," *FEMS Immunology and Medical Microbiology*, vol. 39, no. 1, pp. 17–22, 2003.

[60] M. Wainwright, D. A. Phoenix, J. Marland, D. R. A. Wareing, and F. J. Bolton, "A study of photobactericidal activity in the phenothiazinium series," *FEMS Immunology and Medical Microbiology*, vol. 19, no. 1, pp. 75–80, 1997.

[61] A. P. Castano, T. N. Demidova, and M. R. Hamblin, "Mechanisms in photodynamic therapy: part one—photosensitizers, photochemistry and cellular localization," *Photodiagnosis and Photodynamic Therapy*, vol. 1, no. 4, pp. 279–293, 2004.

[62] K. J. Mellish, R. D. Cox, D. I. Vernon, J. Griffiths, and S. B. Brown, "*In vitro* photodynamic activity of a series of methylene blue analogues," *Photochemistry and Photobiology*, vol. 75, no. 4, pp. 392–397, 2002.

[63] M. Wainwright, D. A. Phoenix, L. Rice, S. M. Burrow, and J. Waring, "Increased cytotoxicity and phototoxicity in the methylene blue series via chromophore methylation," *Journal of Photochemistry and Photobiology B: Biology*, vol. 40, no. 3, pp. 233–239, 1997.

[64] S. S. Stylli and A. H. Kaye, "Photodynamic therapy of cerebral glioma—a review part I—a biological basis," *Journal of Clinical Neuroscience*, vol. 13, no. 6, pp. 615–625, 2006.

[65] R. G. Pearson, "The electronic chemical potential and chemical hardness," *Journal of Molecular Structure: THEOCHEM*, vol. 255, pp. 261–270, 1992.

[66] R. G. Parr, L. v. Szentpály, and S. Liu, "Electrophilicity index," *Journal of the American Chemical Society*, vol. 121, no. 9, pp. 1922–1924, 1999.